

NRC Publications Archive Archives des publications du CNRC

Artifact removal in FD-OCT with a B-M mode scanning technique: condition on the transverse step

Vergnole, Sébastien; Lamouche, Guy

This publication could be one of several versions: author's original, accepted manuscript or the publisher's version. / La version de cette publication peut être l'une des suivantes : la version prépublication de l'auteur, la version acceptée du manuscrit ou la version de l'éditeur.

For the publisher's version, please access the DOI link below. / Pour consulter la version de l'éditeur, utilisez le lien DOI ci-dessous.

Publisher's version / Version de l'éditeur:

<https://doi.org/10.1117/12.808283>

Optical Coherence Tomography and Coherence Domain Optical Methods in Biomedicine XIII, pp. 71682M-1-71682M-8, 2009-02

NRC Publications Archive Record / Notice des Archives des publications du CNRC :

<https://nrc-publications.canada.ca/eng/view/object/?id=4252a7ba-6a22-4dab-bf3f-24f0ddedc478>

<https://publications-cnrc.canada.ca/fra/voir/objet/?id=4252a7ba-6a22-4dab-bf3f-24f0ddedc478>

Access and use of this website and the material on it are subject to the Terms and Conditions set forth at

<https://nrc-publications.canada.ca/eng/copyright>

READ THESE TERMS AND CONDITIONS CAREFULLY BEFORE USING THIS WEBSITE.

L'accès à ce site Web et l'utilisation de son contenu sont assujettis aux conditions présentées dans le site

<https://publications-cnrc.canada.ca/fra/droits>

LISEZ CES CONDITIONS ATTENTIVEMENT AVANT D'UTILISER CE SITE WEB.

Questions? Contact the NRC Publications Archive team at

PublicationsArchive-ArchivesPublications@nrc-cnrc.gc.ca. If you wish to email the authors directly, please see the first page of the publication for their contact information.

Vous avez des questions? Nous pouvons vous aider. Pour communiquer directement avec un auteur, consultez la première page de la revue dans laquelle son article a été publié afin de trouver ses coordonnées. Si vous n'arrivez pas à les repérer, communiquez avec nous à PublicationsArchive-ArchivesPublications@nrc-cnrc.gc.ca.

Artifact removal in FD-OCT with a B-M mode scanning technique: Condition on the transverse step

Sébastien Vergnole and Guy Lamouche

Industrial Materials Institute, National Research Council, 75 bd. de Mortagne, Boucherville,
QC, J4B 6Y4, Canada

ABSTRACT

One of the main drawbacks of Fourier-domain optical coherence tomography is its inability to differentiate between positive and negative locations relative to the zero-delay position. In the recently proposed B-M mode scanning technique, these artifacts are removed by introducing a transverse modulation between successive A-scans followed by a Fourier filtering in the transverse direction. This paper deals with the relation between the transverse step size and the efficiency of artifact removal. This relation is illustrated with measurements performed on an onion with different transverse step sizes and different focusing optics. These experimental results are used to support a proposed criterion for the transverse step. The criterion aims at insuring efficient artifact removal while limiting the amount of oversampling in the transverse scan.

Keywords: Optical Coherence Tomography, Swept Source OCT, Depth Ambiguity, B-M mode scanning, Transverse step

1. INTRODUCTION

In Fourier-Domain optical coherence tomography (FD-OCT), the spatial information is obtained from the Fourier transform of a real signal acquired at different wavelengths. The resulting Fourier transform is hermitian and one cannot distinguish between the positive and negative locations around the zero-delay position (mirror artifact). To remove this depth degeneracy, many recent papers proposed various implementations of the B-M mode scanning technique. The latter was first introduced by Yasuno et al.¹ for spectral domain OCT (SD-OCT). It consists in adding a variable phase shift during the transverse scan while A-scans are recorded. The complex OCT signal is then obtained by first performing a Fourier analysis in the transverse direction. An inverse Fourier transform in the axial direction of the resulting complex OCT signal then provides the depth profile free from artifacts. This can be seen as an extension of the phase-shifting approach,²⁻⁴ but with a more robust processing. Methods proposed to introduce the phase shifts involve piezoelectric transducers,^{1,5,6} off-axis galvanometer scanner,⁷⁻⁹ or electro-optic modulator.¹⁰ We proposed an approach using a piezoelectric fiber stretcher (PFS) to generate discrete phase steps between successive A-scans at a high rate.¹¹

When using B-M mode scanning to remove artifacts, the optimal phase-shift between successive A-scans is $\pi/2$.^{1,8,9,11} The phase can be varied continuously or in a stepwise manner. To further insure efficient artifact removal, transverse variations between adjacent A-scans must be small. This leads to an upper limit on the transverse step size. This problem is only addressed to a certain extent in the published papers. In Ref. 8, the authors state that the total width of the transverse spectral content must not exceed half of the Fourier space defined by the transverse step size. They conclude that the transverse spacing between two A-scans must not exceed the illuminating beam spot size. In Refs. 6 and 7, the authors rely experimentally on 4 to 5 measurements over the illuminating spot size but without providing a detailed explanation. In Ref. 9, based on a short discussion, the authors require that the transverse step size must be much smaller than of the illuminating spot size divided by four. In many of the discussions, the criterion is based on the transverse step size relative to the transverse speckle size. This speckle size is often erroneously assumed equal to the illuminating spot size. In reality, it is smaller due to the collection optics and due to the interference between the many scatterers

Further author information: (Send correspondence to S.V.)

S.V.: E-mail: Sebastien.Vergnole@cnrc-nrc.gc.ca, Telephone: 1 450 641 5137

contained in the probe volume for a biological tissue.¹² In Ref. 11, we proposed a condition on the transverse step relative to the true speckle size. In the current paper, we further study this condition.

We first review our experimental setup for B-M mode scanning using a piezoelectric fiber stretcher along with the signal processing leading to artifact removal. The influence of the transverse step is then illustrated by presenting measurements performed on an onion with various illuminating spot sizes. These images are analyzed by proposing a ratio to quantify what appears qualitatively acceptable for artifact removal. After a short discussion on the transverse spatial Fourier content of the images, we propose a criterion for the transverse step size. This criterion aims at insuring efficient artifact removal while avoiding too much oversampling in the transverse scan. The relevant point of this paper is that this criterion rely not only on theoretical developments but also on various experimental measurements.

2. PIEZOELECTRIC FIBER STRETCHER SS-OCT CONFIGURATION

2.1. Experimental setup

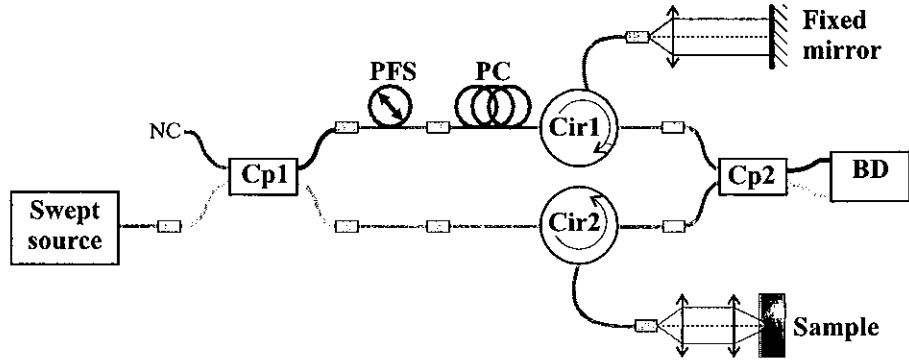


Figure 1. SS-OCT setup. Cp1 and Cp2: couplers, PFS: Piezoelectric Fiber Stretcher, PC: Polarization Controller, Cir1 and Cir2: Circulators, BD: Balanced Detection.

Figure 1 shows our SS-OCT setup that includes a PFS to achieve B-M mode scanning. It is a Mach-Zehnder fiber-based interferometer. The source is a Thorlabs swept-source with a 1325 nm center wavelength and a 85 nm bandwidth (FWHM). The theoretical axial resolution is $\delta z = 9.1 \mu\text{m}$ in air. The wavelength is swept at a repetition rate of 16 kHz alternately in forward and backward directions. In the current work, A-scans are acquired at a reduced rate of 8 kHz by working only with the forward sweeps of the source. The setup is fitted with a PFS from Optiphase (*PZ1-STD-FC/APC*). This device consists of 10 meters of fiber wound around a cylindrical piezoelectric transducer. The PFS drive signal is adjusted to provide a $\pi/2$ phase shift between two successive A-scans.

2.2. Signal processing

The signal processing for artifact removal with B-M mode scanning is well described in the various references. We illustrate it in the simple case for which the sample arm contains a reflective surface. In that case, a B-scan is obtained from the interferometric signal is $i(x, \nu) = k_0 + \cos(k_x x + k_\nu \nu)$ where k_0 is a constant that includes the autocorrelation terms, k_x is linked with the phase shift introduced by the PFS, x is the transverse position, k_ν is linked with the wavelength sweeping of the source, and ν is the optical frequency. We first compute the Fourier transform of $i(x, \nu)$ along the x transverse direction:

$$I(u, \nu) = k_0 \delta(u) + \frac{1}{2} \delta(u - k_x) \cdot e^{-ik_\nu \nu} + \frac{1}{2} \delta(u + k_x) \cdot e^{ik_\nu \nu} , \quad (1)$$

where u is the spatial frequency (Fourier conjugate of x), $k_0 \delta(u)$ is the dc component, the second term on the right hand side is the OCT data, and the last term is the complex conjugate of the second one. A high-pass

filtering with a rectangular window is then performed to keep only the data corresponding to the OCT signal to yield: $\hat{I}(u, \nu) = 1/2 \cdot \delta(u - k_x) \cdot e^{-ik_\nu \nu}$. Then, the inverse transverse Fourier transform is evaluated:

$$\hat{i}(x, \nu) = \mathcal{F}_x^{-1}[\hat{I}(u, \nu)] = \frac{1}{2} \cdot e^{-ik_x x} \cdot e^{-ik_\nu \nu} . \quad (2)$$

Finally, as usually performed in FD-OCT, the axial inverse Fourier transform is evaluated:

$$\hat{I}(x, z) = \mathcal{F}_z^{-1}[\hat{i}(x, \nu)] = \frac{1}{2} \cdot e^{-ik_x x} \cdot \delta(z - k_\nu) , \quad (3)$$

where z is the Fourier conjugate of ν and corresponds to the depth position. It must be noted that we display the OCT image by computing $20 \cdot \log(|\hat{I}(x, z)|)$.

3. IMAGE ANALYSIS

3.1. Experimental results

Figure 2 presents images of an onion after artifact removal obtained with various focusing optics and various transverse step sizes. The illuminating spot size was varied by first collimating the output of the optical fiber to 2 mm in diameter and then focusing it with lenses with different focal lengths $f = 14.5, 25.6$ and 48.0 mm. As the focal length increases, the spot size increases, so does the speckle size. The various transverse step sizes δx for the measurements were 1, 2, 4, and 6 μm . To better appreciate the efficiency of artifact removal, the onion was placed below the zero delay position in order to separate the true image from its mirror counterpart. The images obtained after processing are presented as an array in Fig. 2, the transverse step size increasing from left to right and the focal length increasing in the downward direction. A qualitative observation concludes that images 2(c), 2(d) and 2(h) show very poor artifact removal.

3.2. Artifact removal efficiency

To better appreciate the artifact attenuation efficiency, we need a more quantitative analysis. We propose a ratio computed in the following way:

1. Split image around the zero delay position.
2. Identify the bottom part as the real image.
3. Invert vertically the upper part and identify it as the mirror image.
4. Keep only 5 % of the points with the highest amplitude for each transverse line in the original and the mirror images.
5. Compute the average of these points for each transverse line in both the original and mirror images.
6. Compute the ratio between the averages of the real and mirror images for each distance relative to the zero-delay position.

The ratio was evaluated for each images of Fig. 2 and the results are plotted in Fig. 3. We can now describe in a quantitative manner the qualitative observations about the inefficiency of artifact removal for images 2(c), 2(d) and 2(h). Figure 3 shows that the ratio does not reach 10 dB for these cases. Additionally, artifact removal in image 2(h) is qualitatively on the edge of acceptability. In this case, the ratio is about 15 dB. We thus conclude that the ratio should be 15 dB or more in order to provide a visually acceptable mirror artifact removal.

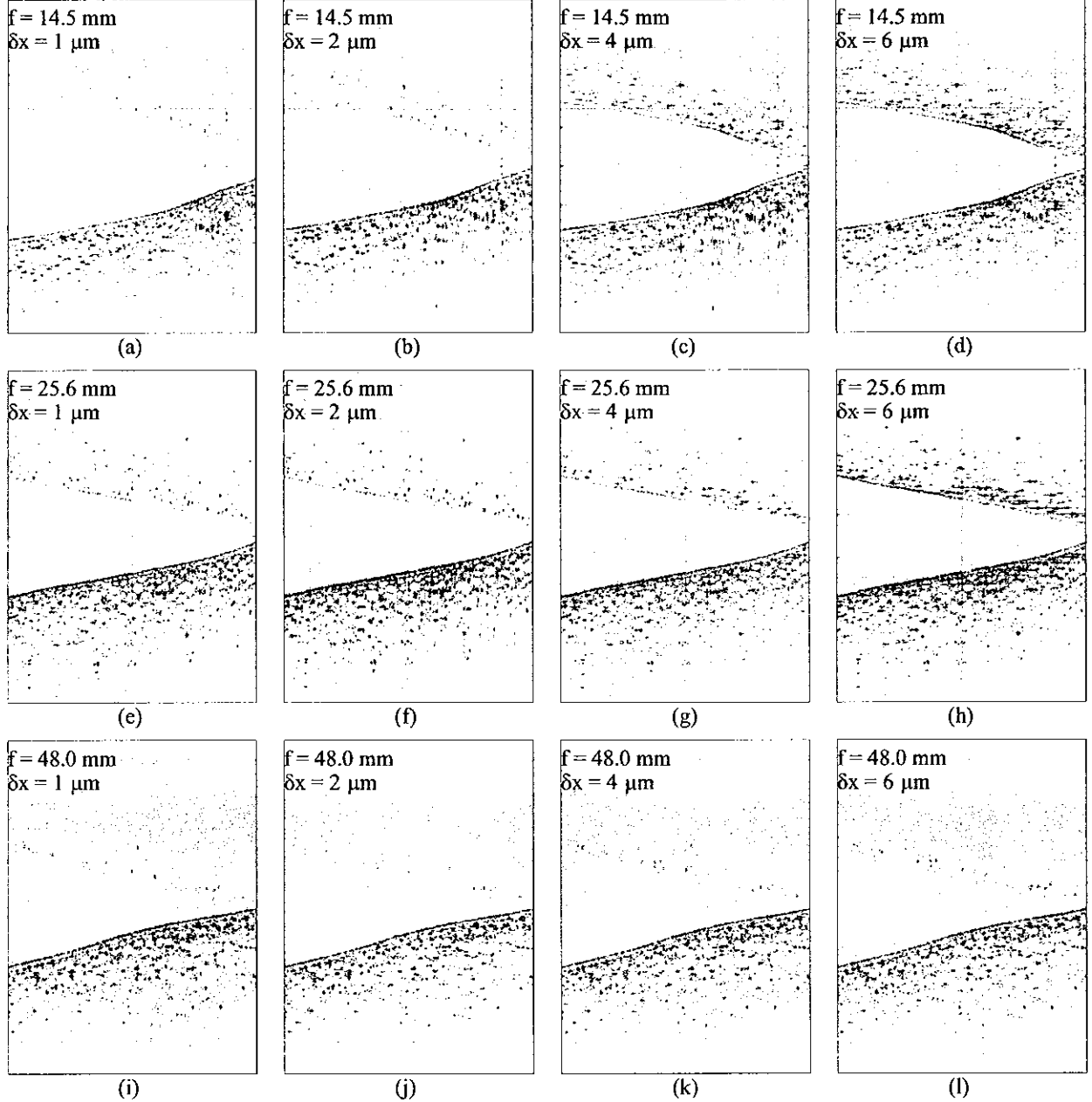


Figure 2. Onion images for different focusing optics and different steps. The dynamic range here is 30 dB.

3.3. Transverse Fourier transform

We have defined a quantitative criterion to assess the efficiency of artifact removal. This criterion is based on the amplitude of the recorded OCT signal. As usually done in discussions about artifact removal using B-M mode scanning, we now look at the spatial frequency content given by a transverse Fourier transform of the various images. Results are presented in Fig. 4 for one transverse line of each image. A good artifact removal efficiency is expected when the spatial frequency content contains two well separated lobes, one for positive frequencies and one for negative frequencies. For cases with inefficient artifact removal ((c), (d) and (h)), Fig. 4 shows that the lobes are not well separated and that they overlap. This allows the determination of another criterion to

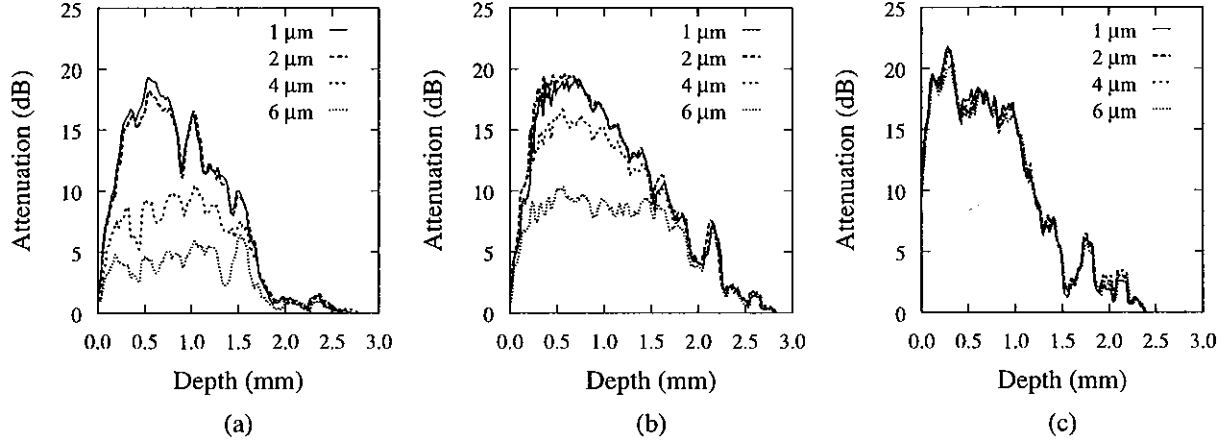


Figure 3. Attenuation ratio as a function of the depth. The ratio is expressed in dB ($20\log$).

insure efficient artifact removal based on the relation between the transverse spatial frequency content and the transverse sampling frequency. The former is determined by the speckle size and the latter by the transverse step size. The criterion thus links the transverse step size to the speckle size. The key point of our paper is that Fourier transforms were evaluated for different illuminating optics and different transverse step sizes. We can thus infer the criterion based on experimental data by taking into account the 15 dB amplitude ratio discussed above. This ratio insures a minimally acceptable artefact removal.

4. CONDITION ON THE TRANSVERSE STEP

To derive a condition on the relation between the transverse step δ_x and the speckle size s , we compare the full width at $1/e$ of the transverse spatial spectrum Δu to the Nyquist frequency $u_{\delta_x} = 1/(2 \cdot \delta_x)$. Based on Figs. 3 and 4, we find that the 15 dB criteria for the OCT amplitude ratio is met when:

$$\Delta u < u_{\delta_x} . \quad (4)$$

Figure 5 illustrates the three different cases $\Delta u \ll u_{\delta_x}$, $\Delta u \sim u_{\delta_x}$, and $\Delta u > u_{\delta_x}$.

We proposed in a previous paper¹¹ the condition $\Delta u < 2 \cdot u_{\delta_x}$. Based on the current experimental data, this proposal was a bit too conservative. It was not optimal because, while insuring a very efficient artefact removal, it implied too much oversampling in the transverse direction. The revised condition in the current paper involves twice less oversampling.

We now rewrite Eq. 4 as a condition on the transverse step δ_x in terms of the speckle size s (full width at $1/e$). We first write the half width at $1/e$ of the spectral content δ_u as a function of the half width at $1/e$ of the speckle size δ_s :

$$\delta u = \frac{1}{\pi \delta_s} . \quad (5)$$

When expressed in terms of the full widths at half-maximum δu and s , this expression takes the form:

$$\Delta u = 2\delta u = \frac{2}{\pi \frac{s}{2}} = \frac{4}{\pi s} . \quad (6)$$

Combining this with the definition of the Nyquist frequency, Eq. 4 becomes:

$$\frac{4}{\pi s} < \frac{1}{2 \delta_x} . \quad (7)$$

We finally obtain the following condition on the transverse step size relative to the speckle size:

$$\delta_x < \frac{\pi s}{8} . \quad (8)$$

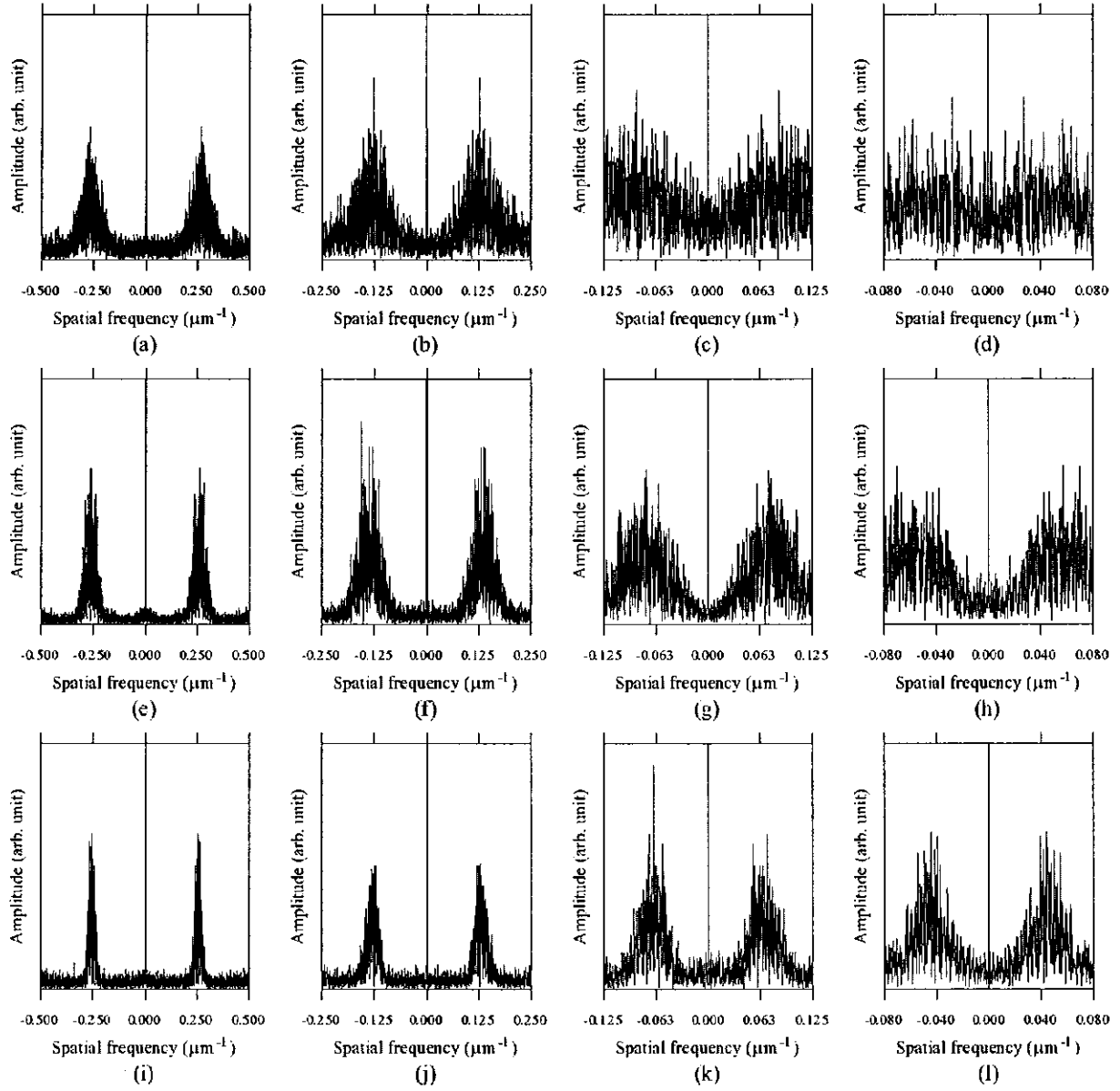


Figure 4. Transverse Fourier transform sections. (a)-(d): $f = 14.5$ mm, (e)-(h): $f = 25.6$ mm, (i)-(l): $f = 48.0$ mm. (a), (e) and (i): $\delta x = 1 \mu\text{m}$, (b), (f) and (j): $\delta x = 2 \mu\text{m}$, (c), (g) and (k): $\delta x = 4 \mu\text{m}$, (d), (h) and (l): $\delta x = 6 \mu\text{m}$.

We must now determine the speckle size in order to further express this condition in terms of the following experimental parameters: the center wavelength λ , the focal length f of the lens, and the beam diameter d (full width at $1/e^2$ for intensity). Two cases must be considered: samples with a high density of scatterers and samples with a low density of scatterers.

For a sample with a low density of scatterers, the speckle size s_{LD} is given by the point-spread function of the illuminating and collecting optics. It takes the form:¹²

$$s_{LD} = \frac{4\lambda f}{\sqrt{2\pi}d} . \quad (9)$$

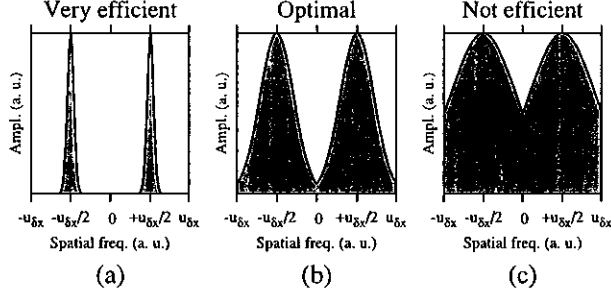


Figure 5. Illustration of different conditions: (a) $\Delta u \ll u_{\delta x}$, (b) $\Delta u \sim u_{\delta x}$ and (c) $\Delta u > u_{\delta x}$.

The condition on the transverse step becomes:

$$\delta x_{LD} < \frac{1}{2\sqrt{2}} \frac{\lambda f}{d} . \quad (10)$$

For a sample with a high density scatterers, the speckle size is further reduced due the coherent addition of the contributions of the scatterers contained within the probe volume.¹² The speckle size takes the form:

$$s_{HD} = 0.68 \frac{4\lambda f}{\sqrt{2}\pi d} . \quad (11)$$

Therefore, the condition for the transverse step size is given by:

$$\delta x_{HD} < \frac{0.68}{2\sqrt{2}} \frac{\lambda f}{d} . \quad (12)$$

This condition should be used for biological tissues since they usually contain a high density of scatterers.

In order to express these conditions differently, we can define the two following parameters:

- the maximum transverse step for a low density of scatterers:

$$\delta x_{maxLD} = \frac{1}{2\sqrt{2}} \frac{\lambda f}{d} , \quad (13)$$

- the maximum transverse step for a high density of scatterers:

$$\delta x_{maxHD} = \frac{0.68}{2\sqrt{2}} \frac{\lambda f}{d} . \quad (14)$$

These values insure a good tradeoff between the artifact removal efficiency and the degree of oversampling.

5. DISCUSSION AND CONCLUSION

For each lenses used in our experiments, Table 1 shows the illumination spot size ($4\lambda f/(\pi d)$), the speckle size from Eq. (11) and the maximum value of the transverse step size as given by Eq. (12). As stated earlier, the collimated beam diameter d was 2 mm. To apply these results to OCT images of an onion, the results for a high density of scatterers were used.

Referring back to Fig. 2, cases (c), (d), and (h) are the only ones which the transverse step size exceeds the allowable value δx_{maxHD} for efficient artifact removal. The maximum value of the transverse step size thus provides an efficient way of insuring the efficiency of artifact removal based on the experimental parameters.

Table 1. Theoretical transverse step limit as a function of the focal lengths used in our experiment.

f (mm)	14.5	25.6	48
Illumination spot size (μm)	12.2	21.6	40.5
s_{HD} (μm)	5.9	10.4	19.5
δx_{maxHD} (μm)	2.3	4.1	7.6

In this paper, we provided a more complete and accurate discussion about the choice of the transverse step with a B-M mode FD-OCT setup. To allow a quantitative assessment of the efficiency of artifact removal, an approach to evaluate the ratio of OCT amplitudes of the real image and its mirror artifact was proposed. This ratio should be better than 15 dB to provide qualitatively acceptable results. A criterion for the transverse step size was then derived. It shows that this transverse step should be lower than $\pi/8$ (≈ 0.40) of the speckle size to get an acceptable artifact removal. When expressed in terms of the more widely used illuminating spot size, the criterion corresponds to about 5 times oversampling with respect to the spot size. We thus proposed a value for the transverse step size that provides a good trade-off between the artifact removal efficiency and the degree of oversampling in the transverse scan, the latter having a direct impact on the measurement time.

ACKNOWLEDGMENTS

The authors thank B. Gauthier for technical support. The authors gratefully acknowledge the financial support of this research by the Genomics and Health Initiative from National Research Council Canada.

REFERENCES

1. Y. Yasuno, S. Makita, T. Endo, G. Aoki, M. Itoh, and T. Yatagai, "Simultaneous b-m-mode scanning method for real-time full-range fourier domain optical coherence tomography," *Applied Optics* **45**(8), pp. 1861–1865, 2006.
2. M. Wojtkowski, A. Kowalczyk, R. Leitgeb, and A. F. Fercher, "Full range complex spectral optical coherence tomography technique in eye imaging," *Optics Letters* **27**(16), pp. 1415–1417, 2002.
3. E. Gtztzinger, M. Pircher, R. A. Leitgeb, and C. K. Hitzenberger, "High speed full range complex spectral domain optical coherence tomography," *Optics Express* **13**(2), pp. 583–594, 2005.
4. A. Bachmann, R. Leitgeb, and T. Lasser, "Heterodyne fourier domain optical coherence tomography for full range probing with high axial resolution," *Opt. Express* **14**(4), pp. 1487–1496, 2006.
5. R. K. Wang, "In vivo full range complex fourier domain optical coherence tomography," *Applied Physics Letters* **90**(5), pp. 054103–3, 2007.
6. R. K. Wang, "Fourier domain optical coherence tomography achieves full range complex imaging in vivo by introducing a carrier frequency during scanning," *Phys Med Biol* **52**(19), pp. 5897–5907, 2007.
7. L. An and R. K. Wang, "Use of a scanner to modulate spatial interferograms for in vivo full-range fourier-domain optical coherence tomography," *Opt. Lett.* **32**(23), pp. 3423–3425, 2007.
8. B. Baumann, M. Pircher, E. Gtztzinger, and C. K. Hitzenberger, "Full range complex spectral domain optical coherence tomography without additional phase shifters," *Opt. Express* **15**(20), pp. 13375–13387, 2007.
9. R. A. Leitgeb, R. Michaely, T. Lasser, and S. C. Sekhar, "Complex ambiguity-free fourier domain optical coherence tomography through transverse scanning," *Opt. Lett.* **32**(23), pp. 3453–3455, 2007.
10. T. Fabritius, S. Makita, M. Yamanari, R. Myllyla, T. Yatagai, and Y. Yasuno, "Full range 1- μm spectral domain optical coherence tomography by using electro-optical phase modulator," in *Coherence Domain Optical Methods and Optical Coherence Tomography in Biomedicine XII*, **6847**, pp. 68471S–6, 2008.
11. S. Vergnole, G. Lamouche, and M. L. Dufour, "Artifact removal in fourier-domain optical coherence tomography with a piezoelectric fiber stretcher," *Opt. Lett.* **33**(7), pp. 732–734, 2008.
12. G. Lamouche, C.-E. Bisillon, S. Vergnole, and J.-P. Monchalain, "On the speckle size in optical coherence tomography," in *Coherence Domain Optical Methods and Optical Coherence Tomography in Biomedicine XII*, J. A. Izatt, J. G. Fujimoto, and V. V. Tuchin, eds., **6847**, p. 684724, 2008.